



Vertebral formula and numerical variations in the spine of the Antarctic and southern South American penguins (Aves: Sphenisciformes)

M. Alejandra Sosa^{1,2}, Carolina Acosta Hospitaleche^{1,3}

¹ *División Paleontología Vertebrados, Museo de La Plata, Facultad de Ciencias Naturales y Museo, Paseo del Bosque s/n, 1900, La Plata, Buenos Aires, Argentina*

² *Universidad Nacional de La Plata, La Plata, Argentina*

³ *CONICET, Buenos Aires, Argentina*

<http://zoobank.org/6A1AB2E0-D962-43A6-8CBA-2E82932478E0>

Corresponding author: M. Alejandra Sosa (alejandrasosa@fnym.unlp.edu.ar)

Academic editor Martin Päckert

Received 13 October 2023

Accepted 22 December 2023

Published 8 March 2024

Citation: Sosa MA, Acosta Hospitaleche C (2024) Vertebral formula and numerical variations in the spine of the Antarctic and southern South American penguins (Aves: Sphenisciformes). *Vertebrate Zoology* 74 209–219. <https://doi.org/10.3897/vz.74.e114112>

Abstract

The vertebral column in tetrapods consists of several constant regions, namely the cervical, thoracic, lumbar, sacral, and caudal regions. Each of these regions is characterized by a specific number of vertebrae, contributing to the overall vertebral formula. Supernumerary and/or missing vertebrae have only been sporadically mentioned for penguins, and the specific vertebral formula is only determined for some non-passerese orders. Variations in the anatomy and vertebral number of South American and Antarctic penguin species are evaluated here. Sixty-six specimens of *Aptenodytes forsteri*, *Pygoscelis adeliae*, *P. antarcticus*, *P. papua*, *Spheniscus magellanicus*, and *Eudyptes chrysocome* were examined to establish the vertebral formula for six South American and Antarctic species, reporting the type and frequency of the variations found in the generalized configuration. We found no intraspecific variation in respect of the number of cervical as well as cervicothoracic vertebrae in all penguin species studied. Intra- and interspecific variation occur in the thoracic, synsacral, and caudal regions comprising 6–7, 13–14 and 5–8 vertebrae, respectively. Particularly, the variations were found in the transitional zones between one region and another and/or between synsacral segments.

Keywords

Axial formula, numerical anomalies, Spheniscidae, synsacral segments, vertebral column

Introduction

The vertebral column is the part of the axial skeleton that protects the spinal cord, provides support and stability to the body, and serves as the origin and insertion of the musculature (Galbusera 2018; Galbusera and Bassani 2019). Each vertebra articulates with its neighbors through the zygapophyses and articular facets of the ver-

tebral body. In birds, adult vertebrae are heterocoelous (i.e., with saddle-shaped articular facets of the vertebral body), except for the thoracic vertebrae of some birds, such as penguins (Sphenisciformes), parrots (Psittaciformes), cormorants (Phalacrocoracidae), some gulls (Laridae), razorbills (Alcidae), and shorebirds (Chara-

driiformes) among others, whose vertebral bodies are opisthocoelous (i.e., the cranial articular facet is convex while the caudal articular facet is concave) (Gadow 1933; Verheyen 1958a; Bellairs and Jenkin 1960).

In tetrapods, in general, the most common and well-known vertebral regions correspond to the cervical, thoracic, lumbar, sacral, and coccygeal or caudal regions (Baumel and Witmer 1993; Narita and Kuratani 2005; Gómez and Pourquié 2009; Galbusera 2018; Galbusera and Bassani 2019). The total number of vertebrae is generally the same within a species, although it is highly variable among different groups of vertebrates. It ranges from six in frogs to hundreds in some fish and snakes (Gómez and Pourquié 2009). In turn, the number of vertebrae within each region is also variable in the different groups, although in mammals, for example, apart from manatees and sloths, cervicals are always seven (Burke et al. 1995; Galis 1999; Narita and Kuratani 2005; Oostra et al. 2005; Böhmer et al. 2019). The combined number of vertebrae that contribute to each of the vertebral column regions has been called axial or vertebral formula (Verheyen 1960; Sawin et al. 1967; Burke et al. 1995; Narita and Kuratani 2005; Gómez and Pourquié 2009).

It is difficult to establish a general vertebral formula in birds because the regionalization of the spine is related to the presence of modifications such as the notarium formed by the fusion of some thoracic vertebrae; the synsacrum formed by ankylosis of thoracic, lumbar, sacral, and caudal vertebrae; and the pygostyle formed by the fusion of the last caudal vertebrae (Baumel and Witmer 1993; Burke et al. 1995; Hiraga et al. 2013). These structures have led to differences between authors when establishing a general vertebral formula since there is no agreement on how to identify each element that constitutes them, especially in the synsacrum (Bellairs and Jenkin 1960; Hiraga et al. 2013). In birds, the total number of vertebrae varies from a minimum of 40 in Passeriformes to a maximum of 60 in swans (Bellairs and Jenkin 1960); the number of cervical varies from nine in parakeets to 25 in swans (Kaiser 2007); and thoracics from five in phalacrocoracids to 11 in cranes (Ono 1980; Hiraga et al. 2013). The synsacrum is formed by ankylosis of 13–14 vertebrae in *Bubo bengalensis* (Franklin, 1831) (Strigidae) (Sridevi et al. 2021) or up to 22 in other birds (Hiraga et al. 2013). The numerical variability found in the literatures for these last two regions mostly depends on whether the first ankylosed vertebra is part of the thoracic region or the synsacrum. Finally, and for similar reasons, the free caudal region presents from five to nine elements, depending on whether the last ankylosed elements are conserved within the caudal region or the synsacrum (Gadow 1933; Bellairs and Jenkin 1969; Hiraga et al. 2013; Pereira 2015; Gofur 2021).

Beyond that, numerical differences have also been found in the same region in several tetrapods. Such is the case of goats and humans among mammals (Simoens et al. 1982; Oostra et al. 2005), or domestic fowl and cranes among domestic and wild birds (Nickel et al. 1977; Hira-

ga et al. 2013), where extra vertebrae, or even absences, have been observed accounting for a lower number of vertebrae for a particular region. These numerical variations occur mainly in the transitional zones between one region and another, for example, in the thoracic-lumbar or lumbar-sacral regions (Simoens et al. 1982; Oostra et al. 2005; Hiraga et al. 2013; Lian et al. 2018), although variations were also reported in the cervical region in cranes (Hiraga et al. 2013). This existing numerical variability within the same species has been called “numerical anomaly” (Oostra et al. 2005), and the causes of its occurrence are still unclear. Although the low genetic diversity can influence the numerical variations of the vertebral column in mammals, among other factors, the cause that can generate this variation in birds is unknown (Hiraga et al. 2013). Additionally, it has been noted that some of these variations can be attributed to differences in ontogenetic stages (Verheyen 1955; Verheyen 1958a, 1958b).

Particularly in penguins, the total number of vertebrae also varies, from 42 in *Eudyptes chrysocome* (Forster, 1781), *Eudyptes chrysolophus* (von Brandt, 1837), *Eudyptula minor* (Forster, 1781), *Pygoscelis papua* (Forster, 1781), *Aptenodytes patagonicus* (Miller, 1778), and *Aptenodytes forsteri* Gray, 1844 (Watson 1883; Shufeldt 1901; Stephan 1979; Sosa and Acosta Hospitaleche 2022) to 43 in *Spheniscus demersus* (Linnaeus, 1758), *Spheniscus magellanicus* (Forster 1781), and *Spheniscus mendiculus* Sundevall, 1871 (Watson 1883). Within each region, some authors mention 13 (Gervais and Alix 1877; Watson 1883; Verheyen 1958a; Stephan 1979; Guinard and Marchand 2010; Guinard et al. 2010; Sosa and Acosta Hospitaleche 2022) or 15 cervical vertebrae (Shufeldt 1901), six (Shufeldt 1901; Verheyen 1958a; Sosa and Acosta Hospitaleche 2022) or eight to nine thoracic vertebrae (Watson 1883; Stephan 1979), 11, 12 or 14 vertebrae in the synsacrum (Watson 1883; Verheyen 1958a; Stephan 1979; Sosa and Acosta Hospitaleche 2022), six to eight free caudals (Watson 1883; Shufeldt 1901; Verheyen 1958a; Stephan 1979; Sosa and Acosta Hospitaleche 2022) in addition to the pygostyle formed by ankylosis of the last four to five (Verheyen 1958a; Sosa and Acosta Hospitaleche 2022), or six to seven caudal vertebrae (Stephan 1979). Two cervicothoracic vertebrae were recently described in penguins (Jadwiszczak 2014; Sosa and Acosta Hospitaleche 2022). It should be noted that these elements were previously considered part of the cervical or the thoracic regions, depending on the author (Watson 1883; Shufeldt 1901; Verheyen 1958a; Stephan 1979).

Recently, an extra vertebra in the thoracic region was detected in a specimen of *Aptenodytes forsteri* (Sosa and Acosta Hospitaleche 2022). Starting from that, we explored the variation in the vertebral column of other penguin species. This work aims to establish the anatomy, the general vertebral formula and its variations in the different penguin species examined. In addition, the configuration of the synsacrum, the most problematic elements in the vertebral count, and its degree of fusion to the pelvic girdle in the different species were analyzed.

Materials and methods

The vertebral column of 66 specimens of six South American and Antarctic penguin species, housed in the collections of the Vertebrate Zoology Division of the Museo Argentino de Ciencias Naturales Bernardino Rivadavia (MACN-Or) of the Ciudad Autónoma de Buenos Aires and the Ornithological Section of the Museo de La Plata (MLP-ORN), La Plata, were analyzed. The sample includes the emperor penguin *Aptenodytes forsteri* (n = 3), Adélie penguin *Pygoscelis adeliae* (Hombron and Jacquinot, 1841) (n = 20), chinstrap penguin *Pygoscelis antarcticus* (Forster, 1781) (n = 1), gentoo penguin *Pygoscelis papua* (n = 9), Magellanic penguin *Spheniscus magellanicus* (n = 32), and rockhopper penguin *Eudyptes chrysocome* (n = 1) (see Table S1). Only subadult and adult penguins were selected based on their fully development of vertebrae, allowing precise allocation within vertebral column regions. Specimen ages were determined following Sosa and Acosta Hospitaleche (2022).

The number of vertebrae was determined by counting each individual, morphologically identifying the regions as follows. Cervical (C): the ribs are fused to the vertebrae, they have a foramen transversarium, and the vertebral body is heterocoelus; cervicothoracic (CT): the ribs are not fused to the vertebrae but do not articulate with the sternum, and the vertebral body is heterocoelus; thoracic (T): the ribs are not fused to the vertebrae and articulate with the sternum, and the vertebral body is opisthocoelus, except for the cranial articular facet of the first thoracic vertebra which is heterocoelus; synsacrum (S): total or partially ankylosed thoracic, lumbar, sacral, and caudal vertebrae; free caudal (Ca): cylindrical vertebral body, triangular vertebral arch, well-developed and rectangular processus transversi, all similar in size and shape; and pygostyle (P): total or partially ossified vertebrae with cylindrical vertebral body compressing and reducing in size caudally.

The vertebral formula for each species was determined as follows: $C_x + CT_x + T_x + S_x + Ca_x + P_{x(x)} = N_{total}$. Capital letters indicate the vertebrae of the cervical, cervicothoracic, thoracic, synsacral, free caudal, and pygostyle regions, respectively. In addition, the subscript “x” shows the number of vertebrae for each region being, for the synsacrum and pygostyle, the total number of ankylosed vertebrae. It is worth noting that for practical purposes, in the total number of vertebrae (N), the pygostyle was counted as a single vertebral element regardless of the number of fused vertebrae indicated in brackets.

The synsacral segments, that form the synsacrum, were analyzed according to Bellairs and Jenkin (1960) and Stephan (1979) and were identified as follows. Thoracic segment (TS): presents articulated ribs; thoracolumbar segment (TLS): presents processus transversi in the first vertebrae and processus transversi and processus costales in the last vertebrae; lumbar segment (LS): presents only processus transversi; sacral segment (SS): presents well-developed processus transversi and processus costales; and caudal segment (CS): presents robust pro-

cessus transversi. For each species, the fusion or not of the synsacrum with the pelvic girdle was also analyzed.

Results

The vertebral column across all examined penguin species demonstrates a consistent configuration, yet our scrutiny reveals subtle distinctions in the presence, absence, or developmental degree of specific processes, as well as variations in the number of elements within each region.

The subsequent section underscores both intra- and interspecific morphological variations, offering a detailed examination of the penguin vertebral column. Our focus centers on the vertebral formula providing an overview of numerical variations within each region.

Morphological descriptions

Cervical vertebrae. The processus ventralis corporis appears from C2 to C4 in *Aptenodytes forsteri* (Fig. 1A), *Pygoscelis papua*, *Spheniscus magellanicus*, and from C2 to C3 in *Pygoscelis adeliae*. Subsequently, this process manifests again from C10 to C13 in *A. forsteri*, *P. adeliae*, *Pygoscelis antarcticus*, *S. magellanicus* and *Eudyptes chrysocome*. In *P. papua* and a specimen of *P. adeliae* (MLP-ORN 15475), it is observed between C9 and C13. The processus carotici develop from C5 to C9 in *A. forsteri* (Fig. 1B), and *S. magellanicus*, from C4 to C8 or C9 in *P. adeliae*, from C5 to C8 in *P. papua* and from C7 to C9 in *E. chrysocome*. The processus costales exhibit a consistent short and spine-like structure across all specimens (Fig. 1C). The processus transversi are slightly developed up to C11 and extend laterodorsally further from C11 to C13 (Fig. 1D) in *A. forsteri*, *P. adeliae*, *P. papua*, *S. magellanicus*, and *E. chrysocome*. In the C13 of *P. antarcticus*, these processus are uniquely dorsally curved. Lastly, the processus spinosus is observed from C2 to C6 and from C12 to C13 in all specimens (Fig. 1D).

Cervicothoracic vertebrae. The vertebral body exhibits subtle variations, being slightly rectangular in *A. forsteri* and quadrangular in the remaining species (Fig. 1E–I). In CT1, the processus ventralis corporis is simple with two well-defined alae cristae ventrales. However, in CT2 it is bifurcated in all species. Both vertebrae have a deep fovea cranioventralis and a well-developed processus transversi, with a rounded and small eminentiae costolaterales. The processus spinosus assumes a quadrangular, flattened structure, covering the entire length of the vertebral arch in all species. Notably, in CT1 of *A. forsteri*, it presents a shorter length and a midline position on the vertebral arch.

Thoracic vertebrae. All vertebrae are opisthocoelus, but the cranial articular facet of T1 acquires a saddle-shape in all species. The processus ventralis corporis decreases

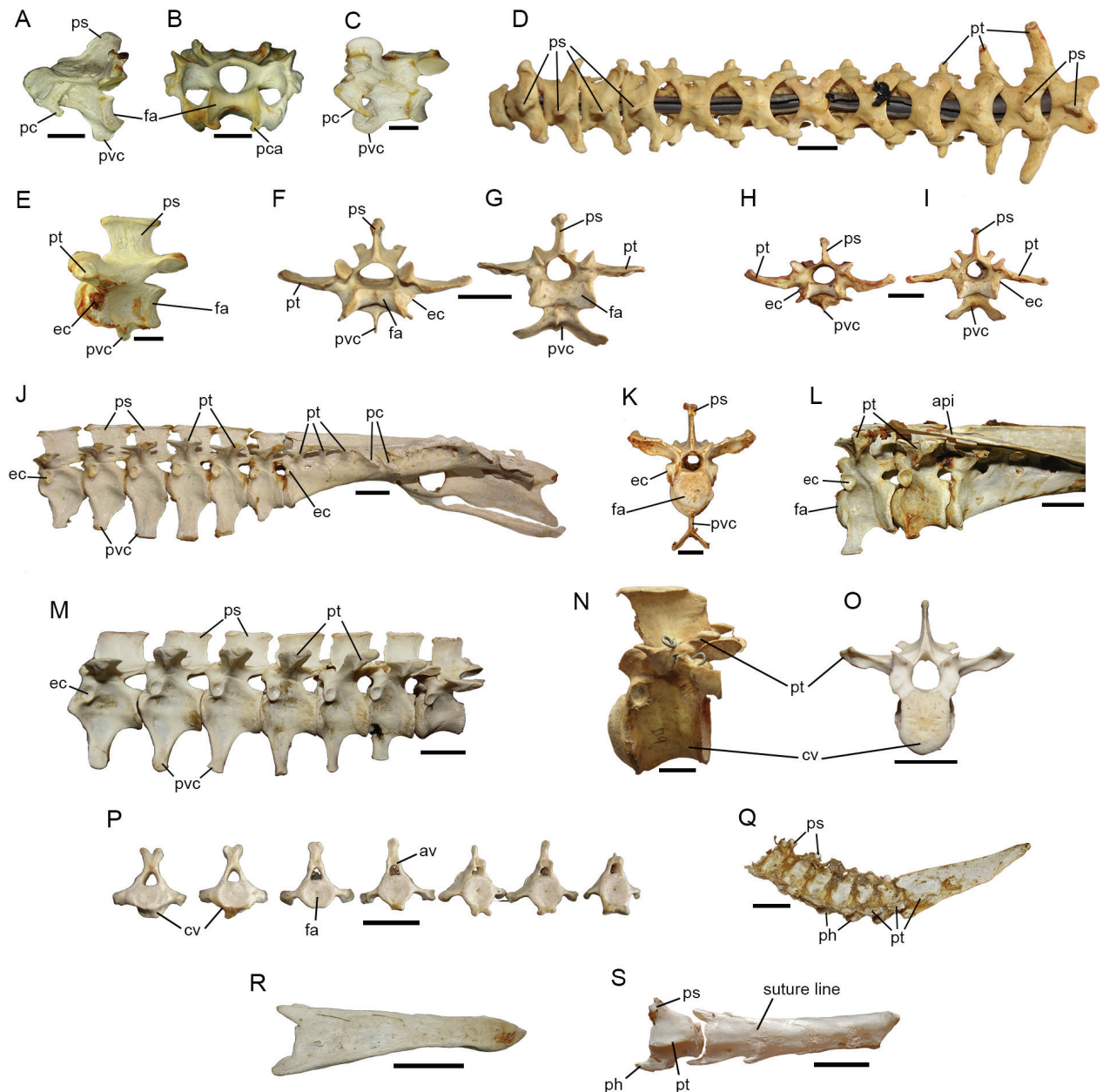


Figure 1. General aspects: **A** C4 in left lateral view, *Aptenodytes forsteri* (MLP-ORN 15192); **B** C8 in cranial view, *Aptenodytes forsteri* (MLP-ORN 15192); **C** C11 in left lateral view, *Aptenodytes forsteri* (MLP-ORN 15192); **D** C1–C13 in dorsal view, *Pygoscelis papua* (MLP-ORN 783); **E** CT1 in left lateral view, *Aptenodytes forsteri* (MLP-ORN 15192); **F** CT1 in cranial view, *Pygoscelis adeliae* (MLP-ORN 1134); **G** CT2 in cranial view, *Pygoscelis adeliae* (MLP-ORN 1134); **H** CT1 in cranial view, *Spheniscus magellanicus* (MLP-ORN 1598); **I** CT2 in cranial view, *Spheniscus magellanicus* (MLP-ORN 1598); **J** T1–T6 and synsacrum in left lateral view, *Eudyptes chrysocome* (MLP-ORN 1596); **K** T2 in cranial view, *Aptenodytes forsteri* (MLP-ORN 15192); **L** T6, T7 and the cranial end of the synsacrum in left lateral view, *Pygoscelis adeliae* (MACN-Or 68557); **M** T1–T7 in left lateral view, *Spheniscus magellanicus* (MACN-Or 71167); **N** T7 in left lateral view, *Aptenodytes forsteri* (MLP-ORN 15192); **O** T7 in cranial view, *Spheniscus magellanicus* (MACN-Or 71167); **P** Ca1–Ca7 in cranial view, *Eudyptes chrysocome* (MLP-ORN 1596); **Q** Ca1–Ca6 and pygostyle in left lateral view, *Pygoscelis antarcticus* (MLP-ORN 1138). **R** pygostyle in left lateral view, *Eudyptes chrysocome* (MLP-ORN 1596), adult; **S** pygostyle in left lateral view, *Spheniscus magellanicus* (MACN-Or 71167), juvenile, where the first vertebra is still unfused. Abbreviations: api – ala praeacetabularis ilii; av – arcus vertebrae; cv – corpus vertebrae; ec – eminentia costolateralis; fa – facies articularis; pc – processus costalis; pca – processus caroticus; ph – processus haemalis; ps – processus spinosus; pt – processus transversus; pvc – processus ventralis corporis. Scale bar: 10 mm.

cranio-caudally in length (Fig. 1J). It is bifurcated (Fig. 1K) from T1 to T3 transitioning to a simple form from T4 to T6 in *A. forsteri*, *P. adeliae*, *P. antarcticus*, *E. chrysocome*, and some specimens of *S. magellanicus*. In contrast, other specimens of *S. magellanicus* and *P. papua*,

exhibit bifurcated processus ventralis corporis in T1 and T2 and simple processes from T3 to T6. The eminentia costolaterales, rounded in shape, are prominently developed in *A. forsteri*, but smaller in the remaining species. The processus transversi are quadrangular, dorsoventrally

Table 1. General vertebral formula for the six species analyzed. Abbreviations: C – Cervical region; CT – Cervicothoracic region; T – Thoracic region; S – Sinsacrum; Ca – Free caudal region; P – Pygostyle.

Species	Vertebral formula
<i>Aptenodytes forsteri</i>	$C_{13} + CT_2 + T_6 + S_{13} + Ca_7 + P_{1(5)} = 42$
<i>Eudyptes chrysocome</i>	$C_{13} + CT_2 + T_6 + S_{13} + Ca_7 + P_{1(5)} = 42$
<i>Pygoscelis adeliae</i>	$C_{13} + CT_2 + T_6 + S_{14} + Ca_6 + P_{1(5)} = 42$
<i>Pygoscelis antarcticus</i>	$C_{13} + CT_2 + T_6 + S_{14} + Ca_6 + P_{1(5)} = 42$
<i>Pygoscelis papua</i>	$C_{13} + CT_2 + T_6 + S_{14} + Ca_6 + P_{1(5)} = 42$
<i>Spheniscus magellanicus</i>	$C_{13} + CT_2 + T_6 + S_{13} + Ca_6 + P_{1(5)} = 41$

flattened and laterally expanded. The processus spinosus is well-developed, quadrangular, compressed, and covers the entire length of the vertebral arch. Noteworthy variations occur when T5 is the last thoracic, resulting in a reduced and simple processus ventralis corporis. Conversely, when the T7 is present (Fig. 1L–O), this process is absent, while the dorsally curved and well-developed processus transversi make contact with the alae praeacetabulares ilii of the pelvic girdle.

Sinsacrum. The sinsacral body, robust and slightly curved, is divided into the classical five segments (Fig. 1J): TS, TLS, LS, SS, and CS. Between S1 and S4, the sinsacral body is strongly compressed, a feature consistently observed across most species, with *P. papua* displaying a slightly less pronounced compression. From S4 to the caudal end, the sinsacrum exhibits dorso-ventral depression, widening between S4 and S10, and subsequently decreasing in size from S11 to the caudal end. The processus transversi exhibit variability, being long in S1 and S2 and gradually decreasing in length until the CS. In the CS, these processes acquire a rectangular shape and extend laterally.

The sulcus ventralis sinsacri varies in depth and width, being deep and broad in *E. chrysocome*, narrow in *P. adeliae*, *P. antarcticus*, *P. papua*, and *S. magellanicus*, and absent in *A. forsteri*. The processus costales are developed between S4–S6 in *S. magellanicus*, *P. adeliae*, *A. forsteri*, *P. papua*, and *P. antarcticus*, S5–S6 in *E. chrysocome*, and then in S8–S9 in *E. chrysocome*, S9–S10 in *S. magellanicus*, and *P. adeliae*, and S10–S11 in *A. forsteri*, *P. papua*, and *P. antarcticus*. The crista spinosa sinsacri, compressed at the cranial end, decreases in height cranio-caudally toward the last sinsacral vertebra.

A significant interspecific variation is observed in the fusion of the sinsacrum to the pelvic girdle. *Aptenodytes forsteri*, *S. magellanicus*, and *E. chrysocome* do not exhibit fusion. On the contrary, in *P. adeliae* fusion occurs to varying degrees, involving the last two vertebrae of the TLS, all vertebrae of the LS and SS, and the first two (e.g., MLP-ORN 15476) or three (MACN-Or 68826) vertebrae of the CS. *Pygoscelis antarcticus* presents full fusion, with the processus transversi and the processus costales of all sinsacral vertebrae fused to the pelvic girdle. In *P. papua*, fusion affects the last three vertebrae of the TLS, all vertebrae of the LS and SS, and the first (MACN-Or 68596) or second (MLP-ORN 14767) vertebrae of the CS.

Free caudal vertebrae. They exhibit a cylindrical vertebral body (Fig. 1P, Q) characterized by slightly concave or flat articular facets and a triangular vertebral arch. A bifid processus spinosus is observed in varying segments across different penguin species. In *E. chrysocome* it occurs from Ca1 to Ca3, in some specimens (e.g. MLP-ORN 15138) of *P. adeliae* and in *P. papua* from Ca1 to Ca4. Notably, in *A. forsteri*, *P. antarcticus*, and *S. magellanicus*, as well as some specimens (MACN-Or 68558) of *P. adeliae*, the bifid processus spinosus is observed from Ca1 to Ca5. Conversely, in the remaining free caudal vertebrae, the processus spinosus assumes a simple form. The processus haemalis appear consistently from Ca4 to the last free caudal vertebra. Robust and quadrangular, the processus transversi exhibit a consistent morphology across all free caudal vertebrae.

Pygostyle. It results from the ankylosis of five caudal vertebrae, progressively decreasing cranio-caudally in size, forming a triangular single structure (Fig. 1Q, R). In subadults, the initial vertebra of the pygostyle remains unfused, displaying a cylindrical vertebral body with a well-developed processus haemalis, a poorly developed processus spinosus, and weakly (or absent) processus transversi (Fig. 1S).

Vertebral formula and numerical variation (Table 1)

The cervical and cervicothoracic regions exhibits a consistent configuration across all species. In the majority of species, the thoracic region typically comprises six vertebrae; however, exceptions are noted. Specifically, T7 is present in MLP-ORN 1586 (*A. forsteri*) and MACN-Or 71167 (*S. magellanicus*). On the other hand, specimens MACN-Or 73283 (*P. adeliae*) and MLP-ORN 135 (*S. magellanicus*) display a unique variation, featuring only five thoracic vertebrae.

The sinsacrum comprises 13 ankylosed vertebrae in *A. forsteri*, *E. chrysocome*, 19 specimens of *S. magellanicus*, and two specimens of *P. adeliae* (MACN-Or 68557 and MLP-ORN 15137), as well as one specimen of *P. papua* (MLP-ORN 15410). In contrast, *P. adeliae*, *P. antarcticus*, *P. papua*, and 11 specimens of *S. magellanicus* exhibit a sinsacrum formed by 14 ankylosed vertebrae.

Additionally, all species exhibit five discernible sinsacral segments, with variations in the number of vertebrae. In *S. magellanicus* and *P. adeliae* (Fig. 2A, B),

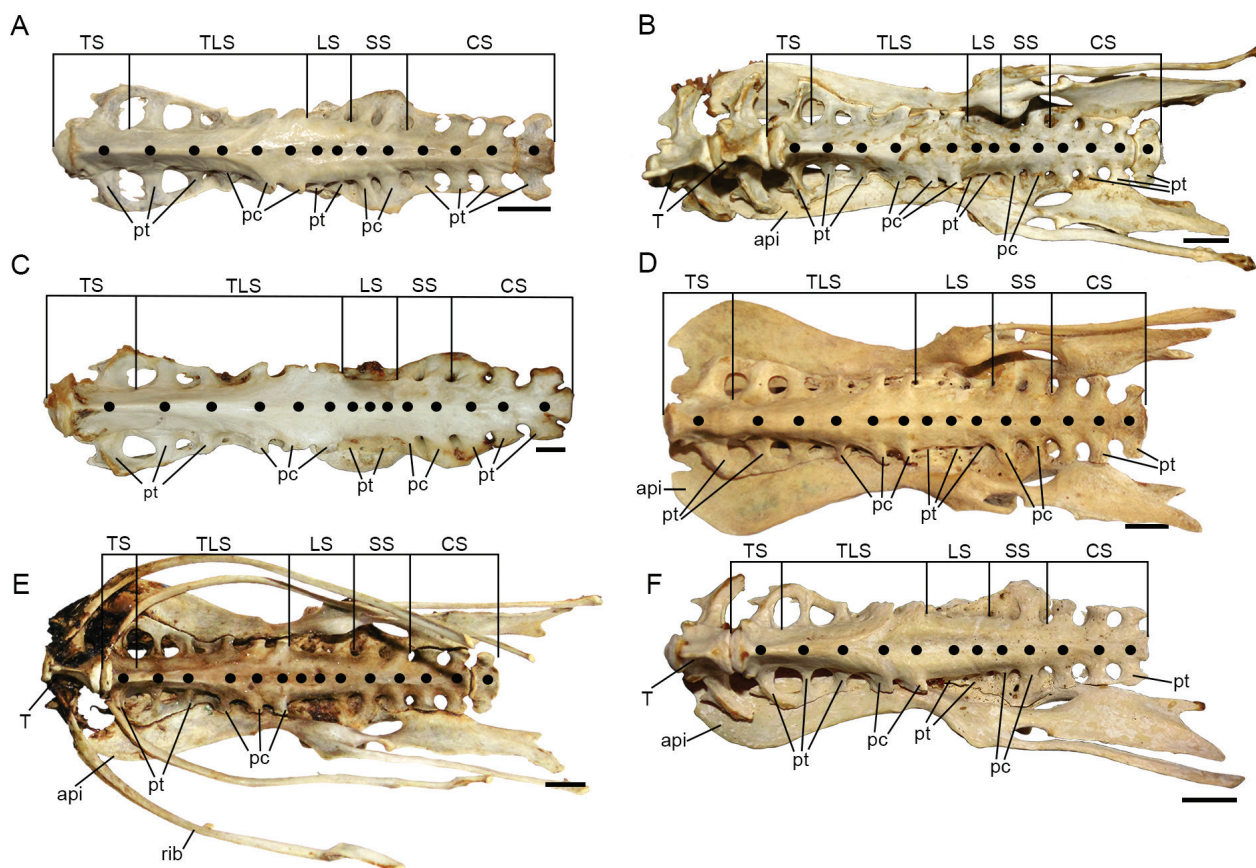


Figure 2. Synsacra and pelves (in B, D–F) in ventral view. **A** *Spheniscus magellanicus* (MLP-ORN 1598); **B** *Pygoscelis adeliae* (MACN-Or 68557); **C** *Aptenodytes forsteri* (MLP-ORN 15192); **D** *Pygoscelis papua* (MLP-ORN 783); **E** *Pygoscelis antarcticus* (MLP-ORN 1138); **F** *Eudyptes chrysocome* (MLP-ORN 1596). Synsacral segments: TS – Thoracal Segment; TLS – Thoracolumbar Segment; LS – Lumbar Segment; SS – Sacral Segment; CS – Caudal Segment. Abbreviations: api – ala praeacetabularis ilii; pc – processus costalis; pt – processus transversus; T – thoracic vertebra. Black circles indicate each individual vertebra. Scale bar: 10 mm.

the synsacral configuration is represented as follows: TS: 1, TLS: 5, LS: 2, SS: 2, CS: 4. Conversely in *A. forsteri*, *P. papua*, and *P. antarcticus* (Fig. 2C–E) the configuration is TS: 1, TLS: 5, LS: 3, SS: 2, CS: 3. Meanwhile, in *E. chrysocome* (Fig. 2F) the configuration is TS: 1, TLS: 4, LS: 2, SS: 2, CS: 3.

Variation within different segments are also evident. In *P. adeliae* the observed variation includes three vertebrae in the CS (specimens MLP-ORN 15137 and MACN-Or 68557), and three vertebrae in both LS and CS (specimen MACN-Or 73283). *P. papua* exhibits variations, such as in MLP-ORN 14921, which has two TS vertebrae (identified by the presence of eminentiae costolaterales), and only two TLS with processus costales. Another specimen, MLP-ORN 14900, also displays only two last vertebrae of the TLS with processus costales. MLP-ORN 15410 is characterized by one missing vertebra in the TLS, with only the last two vertebrae of this segment bearing processus costales. In *S. magellanicus*, specimen MACN-Or 73286 features four vertebrae in the TLS, and among specimens with 13 synsacral elements, the absent vertebra corresponds to the CS segment.

The counts of free caudal vertebrae varies, ranging between five (e.g. MLP-ORN 15476 *P. adeliae*), six (e.g. MLP-ORN 1138 *P. antarcticus*), seven (e.g. MLP-ORN

15038 *P. adeliae*, MLP-ORN 14921 *P. papua*, MLP-ORN 949 *S. magellanicus*), or eight (e.g. MLP-ORN 929 *S. magellanicus*). In all species, the pygostyle is elongated and acquires a triangular shape, consistently formed by five vertebrae that fuse during postnatal ontogeny. Notably, the cranialmost vertebra composing the pygostyle is notably sturdier than the others, with shorter processus transversi compared to the free caudal vertebrae, and more expanded processus haemalis. This unique morphology distinguishes this vertebra among other free caudal vertebrae, whether free or already fused to the pygostyle.

Discussion

Morphology and general vertebral formula

The present work examined the complete spine of 66 specimens (Table 2), offering new and updated insights into six species inhabiting Southern South America and Antarctica. The findings represent the first data for *Pygoscelis antarcticus*, and include updated observations that

Table 2. Total number of vertebrae by species and by region, and the number of cases in which the more general total numbers occur, and the number of cases where variations occur. N indicates the total number of specimens analyzed per species.

Species (N)	Condition	Number of cases ^a	Number of vertebrae						Total
			Cervical	Cervico-thoracic	Thoracic	Synsacrum	Free Caudals	Pygo-style	
<i>Aptenodytes forsteri</i> (3)	General	1	13	2	6	13	7	1(5)	42
	Extra vertebra	1	13	2	7	13	7	1(5)	43
<i>Eudyptes chrysocome</i> (1)	General	1	13	2	6	13	7	1(5)	42
<i>Pygoscelis adeliae</i> (20)	General	9	13	2	6	14	6	1(5)	42
	Homeotic transformation	2	13	2	7	13	6	1(5)	42
	Extra vertebra	3	13	2	6	14	7	1(5)	43
	Missing vertebra	1	13	2	5	14	6	1(5)	41
<i>Pygoscelis antarcticus</i> (1)	General	1	13	2	6	14	6	1(5)	42
<i>Pygoscelis papua</i> (9)	General	4	13	2	6	14	6	1(5)	42
	Extra vertebra	1	13	2	6	14	7	1(5)	43
	Missing vertebra	1	13	2	6	13	6	1(5)	41
		2	13	2	6	14	5	1(5)	41
<i>Spheniscus magellanicus</i> (32)	General	10	13	2	6	13	6	1(5)	41
	Homeotic transformation	1	13	2	7	13	5	1(5)	41
	Extra vertebra	8	13	2	6	14	6	1(5)	42
		1	13	2	6	13	7	1(5)	42
		1	13	2	6	13	8	1(5)	43

^a The number of cases does not include those specimens that were incomplete.

expand upon previous knowledge for *Eudyptes chrysocome*, *Pygoscelis papua*, *Pygoscelis adeliae*, *Aptenodytes forsteri*, and *Spheniscus magellanicus* (Watson 1883; Shufeldt 1901; Verheyen 1958a; Stephan 1979; Guinard and Marchand 2010; Guinard et al. 2010; Jadwiszczak 2014; Pereira 2015; Sosa and Acosta Hospitaleche 2022). As a result, the general vertebral formula for the six studied Sphenisciformes species can be established as $C_{13} + CT_2 + T_6 + S_{13/14} + Ca_{6/7} + P_{5(1)} = 41/42$.

Our findings reveal a total number of 42 vertebrae for *E. chrysocome*, *P. papua*, and *A. forsteri*, consistent with previous reports (Watson 1883; Shufeldt 1901; Sosa and Acosta Hospitaleche 2022). Similarly, *P. adeliae* and *P. antarcticus*, not examined by previous authors, also present this same count. *Spheniscus magellanicus* shows a total of 41 vertebrae, contrasting with the 43 elements reported by previous studies (e.g., Watson 1883). This mismatch was also pointed out by Pereira (2015), who counted 42 or 41 vertebrae in different specimens.

The cervical region consistently comprises 13 vertebrae across all analyzed species, aligning with observations by Gervais and Alix (1877), Watson (1883), Verheyen (1958a), Stephan (1979), Guinard and Marchand (2010), Guinard et al. (2010), and Sosa and Acosta Hospitaleche (2022). Morphologically, the cervical vertebrae of the studied penguin species are similar and almost indistinguishable, except for the sturdier vertebrae of the large-bodied species *A. forsteri*. The main differences occurred in the presence/absence of specific structures when comparing different species. For instance, in *A. forsteri*, the processus spinosus is present from C2 to C7 and in C13, whereas in other species, it appears from C2 to C6 and from C12 to C13. Similarly, the processus ventralis corporis is observed from C2 to C4 in *A. forsteri* and *P.*

papua, from C2 to C3 in *P. adeliae*, from C9 to C13 in *P. papua* and *P. adeliae*, and C10 to C13 in *P. adeliae* (again) and *A. forsteri*.

In all species, two cervicothoracic vertebrae, also referred as “transitional” (Fürbringer 1888), were identified. These vertebrae exhibit an intermediate morphology between cervical and thoracic vertebrae. While mentioned and described only by Jadwiszczak (2014) and Sosa and Acosta Hospitaleche (2022) in penguins, other authors include them either within the cervical (Shufeldt 1901; Verheyen 1958a, although the latter recognized their distinct morphology) or thoracic region (Watson 1883; Stephan 1979).

The thoracic vertebrae, characterized by the presence of unfused ribs articulating with the sternum (Baumel and Witmer 1993) appear usually in a number of six. Except by the cranial articular facet of T1, all thoracics are opisthocoelus (see Baumel and Witmer 1993; Verheyen 1958a; Bellairs and Jenkin 1960; Watson 1883; Sosa and Acosta Hospitaleche 2022). Confirming Verheyen (1858a) observations, we noted that the processus ventralis corporis are bifid only in the first two or three thoracic vertebrae.

The first vertebra, ankylosed to the synsacrum and bearing ribs, used to be included in the thoracic region (Watson 1883; Takashima and Mizuma 1981; Hiraga et al. 2013), contributing to variations in vertebrae count across different author criteria (Pereira 2015). Indeed, the synsacrum, with 13–14 vertebrae, is the most variable element in terms of size, robustness, composition, and association with the pelvic girdle. In line with the classifications of Bellairs and Jenkin (1960) and Stephan (1979), the five synsacral segments were identified. Contrary to Watson (1883), in all *Pygoscelis* species, the synsacrum is fused to the pelvic girdle.

Most species, such as *P. adeliae*, *P. antarcticus*, *P. papua*, and *S. magellanicus*, exhibit six free caudal vertebrae. However, seven free caudal vertebrae are counted in *A. forsteri* and *E. chrysocome*. Variations in the number of caudal vertebrae have also been reported in cranes (Gruidae) (Hiraga et al. 2013). The pygostyle resulted as the most conservative element, composed of five vertebrae ankylosed forming a triangular structure in all species described here (see also Felice and O'Connor 2014). However, Verheyen (1958a) identified four to five elements in most of the living penguin species, and Stephan (1979) described six to seven caudal vertebrae constituting the pygostyle.

Numerical variations

Numerical changes in the vertebral series can result from meristic variations, also called numerical anomalies (Verheyen 1858a, 1858b; Verheyen 1960; Oostra et al. 2005), or homeotic transformations. Meristic variations involve alterations in the total number of segments or elements, while homeotic transformations encompass variations in the number and ordinal position of vertebrae within or between regions, or the acquisition of morphology typical of another position in the spine. Importantly, the latter does not necessarily lead to a change in the total number of vertebrae (Bateson 1894; Guinard 2012). Examples of homeotic transformations includes where some lumbar vertebrae adopt the morphology the sacral vertebrae, with modified processus transversi supporting the pelvic girdle (Bateson 1894). While numerical variations in the vertebral column have been extensively studied in humans (Decker 1915; Danforth 1930; Schultz 1947; Bornstein and Peterson 1966; de Beer Kaufman 1974; Cimen and Elden 1999; Oostra et al. 2005; Lian et al. 2018), similar occurrences have been reported in goats (Simoens et al. 1982 and literature cited there), primates (Schultz 1947), salamanders (Bumpus 1897), and rabbits (Sawin et al. 1967). In general, supernumerary vertebrae are most commonly observed in the thoraco-lumbar or lumbo-sacral transition zones (Sawin et al. 1967), although occurrences have been noted in thoracic and lumbar vertebrae (de Beer Kaufman 1974; Hiraga et al. 2013) and even in cervical regions (Hiraga et al. 2013). Various factors contribute to these numerical variations, including sexual differences, responses to different stimuli, genetic variability (Danforth 1930; Borstein and Peterson 1966; Lian et al. 2018), growth and body size due to differences in the number of genes (Sawin 1967 and literature cited there), and population differences (Borstein and Peterson 1966), but not to age differences (Bornstein and Peterson 1966).

We found numerical variabilities in the thoracic, synsacral, and caudal regions among species (Fig. 3). *Aptenodytes forsteri*, *P. adeliae*, *P. papua*, and *S. magellanicus* show numerical anomalies in the thoracic (+1, or -1) or in the caudal (+2, +1, or -1) regions. For instance, one specimen of *A. forsteri* (MLP-ORN 1586) exhibited an additional vertebra (T7), consistent with findings

reported by Sosa and Acosta Hospitaleche (2022) and verified in this study. In the caudal region, additional vertebrae were found in four species: a seventh free caudal in *P. adeliae* (MLP-ORN 15038 and MLP-ORN 14680), *P. papua* (MLP-ORN 14921), and *S. magellanicus* (MLP-ORN 949 and MLP-ORN 950), and an eighth free caudal in one specimen of *S. magellanicus* (MLP-ORN 920). Furthermore, instances of missing vertebrae concerning the generalized vertebral formula were observed, such as in one specimen of *S. magellanicus* (MLP-ORN 1408) with only five thoracic vertebrae, and in *P. papua*, where one vertebra was absent in the TLS of the synsacrum (MLP-ORN 15410), or with only five free caudal vertebrae (MLP-ORN 14669 and MLP-ORN 14610).

The numerical anomalies identified in Sphenisciformes were attributed to ontogenetic causes by Verheyen (1958a). However, it is plausible that homeotic transformations account for the variations observed in the synsacrum among certain penguin species examined in this study. Specifically, in some specimens of *P. adeliae* and *S. magellanicus*, a vertebra from the TLS acquires the morphology of another vertebra from the TS, maintaining the total number of vertebrae for the species. Other examples include cases of *P. adeliae* (MLP-ORN 15137 and MACN-Or 68557) with seven free caudal vertebrae and a missing element in the CS (MLP-ORN 15038 and MLP-ORN 14680 in the two former specimens). Despite this variations, they retain a total of 42 vertebrae, with 13 vertebrae in the synsacrum and one fewer in the CS (MLP-ORN 15137 and MACN-Or 68557), a pattern also observed in the latter two specimens. Remarkably, these two last specimens also develop seven thoracic vertebrae and six free caudals. In the case of *S. magellanicus*, one specimen (MACN-Or 71167) presented a T7 (also mentioned by Pereira (2014) in the 19% of her sample) and a missing free caudal vertebra, but maintain the count of 41 vertebrae, which is typical for the species. All these specimens exhibit the thoracic vertebra corresponding to the TS ankylosed to the synsacrum, eliminating the possibility of confusion arising from the absence of fusion or incomplete ontogenetic development.

Other cases of numerical variation probably caused by homeotic transformations are observed within the synsacrum, characterized by counts of either 13 or 14 vertebrae. These variations predominantly occur in the TLS and CS, although occurrences were also noted in the TS. In one specimen of *P. papua* (MLP-ORN 14921) the TLS displayed an unusual development: the first vertebra exhibited eminentiae costolaterales (like those of the TS), while the last two vertebrae possessed processus costales, a feature typically seen in three vertebrae among the majority of specimens of this species. This specimen presented six thoracic vertebrae and a total of 14 synsacral vertebrae, which aligns with the general count for the species. Another specimen of *P. papua* (MLP-ORN 15410) presented only 13 vertebrae in the synsacrum, with the missing vertebra corresponding to the TLS, where the first two vertebrae displayed processus transversi, while

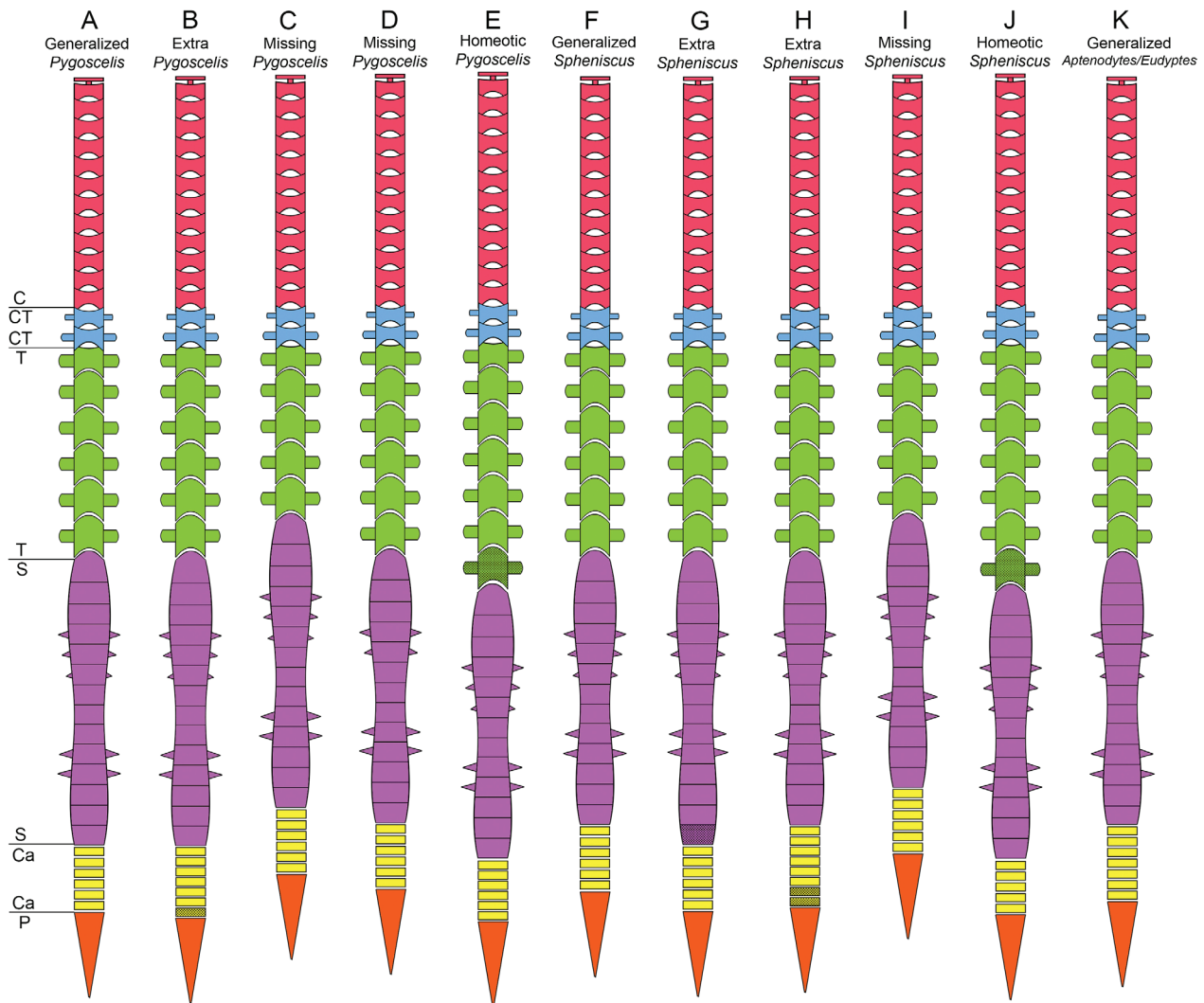


Figure 3. Schematic representation of the vertebral column of penguins representing the general vertebral formula and its numerical variations. **A** General vertebral formula of *Pygoscelis*; **B** Numerical variation with extra vertebrae in the caudal region, e.g. *Pygoscelis papua*; **C** Numerical variations with a missing vertebra in the thoracic region, e.g. *Pygoscelis papua*; **D** Numerical variation with a missing vertebra in the thoracolumbar segment of the synsacrum, e.g. *Pygoscelis papua*; **E** Numerical changes in the thoracic region and the lumbar segment of the synsacrum occur due to homeotic transformations. There is a variation in the number of the vertebrae within regions (an extra thoracic vertebra and a missing vertebra in the lumbar segment of the synsacrum), but not provokes a change in the total number of vertebrae, e.g. *Pygoscelis papua*; **F** General vertebral formula of *Spheniscus*; **G** Numerical variation with an extra vertebra in the caudal segment of the synsacrum, e.g. *Spheniscus magellanicus*; **H** Numerical variation with two extra vertebrae in the free caudal region, e.g. *Spheniscus magellanicus*; **I** Numerical variation with a missing vertebra in the thoracic region, e.g. *Spheniscus magellanicus*; **J** Numerical changes in the thoracic and free caudal region occur due to homeotic transformations. There is a variation in the number of the vertebrae within regions (an extra thoracic vertebra and a missing free caudal vertebra) but not provokes a change in the total number of vertebrae, e.g. *Spheniscus magellanicus*; **K** General vertebral formula of *Aptenodytes/Eudyptes*. Abbreviations: C – cervical vertebrae; CT – cervicothoracic vertebrae; T – thoracic vertebrae; S – synsacrum; Ca – free caudal vertebrae; P – pygostyle.

the last two presented processus costales. Despite this variation, this specimen exhibited six thoracic and six caudal vertebrae, representing the most common count for this species.

The most significant variability in the number and configuration of synsacral vertebrae (ranging from 13 to 14 vertebrae) among penguins was observed in *S. magellanicus*. Specimens with 13 synsacral vertebrae exhibit one missing element in the CS, maintaining the typical total count for the species. However, the specimen MACN-Or 73286 has one vertebra less in the TLS.

Conclusions

The number of vertebral elements of each region in the species analyzed ratifies previous data (e.g., Watson 1883; Stephan 1979; Pereira 2015), considering the differences due to the non-consideration of the cervicothoracic region as such, and the inclusion of the first element of the synsacrum in the thoracic region. Based on the four genera and six species analyzed, we establish the general vertebral formula as $C_{13} + CT_2 + T_6 + S_{13/14} + Ca_{6/7} +$

$P_{5(1)} = 41/42$. The total number is 41 for *S. magellanicus*, and 42 for *A. forsteri*, *P. adeliae*, *P. antarcticus*, *P. papua*, and *E. chrysocome*. Numerical variations, neither restricted to a particular genus or species, nor related to age, were mainly located in the transitional zone between the thoracic region and the synsacrum, and within the synsacrum, in the transitional zone between the segments (TS-TLS, TLS-LS). It could be caused by homeotic or meristic transformations and acquires a lesser magnitude than in other groups of birds (see Hiraga et al. 2013). The causes of this variability are still unknown, and future studies are necessary to expand this information to the remaining penguin species, besides other families of birds, and determine the factors that generate said variation.

Acknowledgements

We are grateful to Yolanda Davies from the “Museo Argentino Bernardino Rivadavia” for kindly receiving MAS in the collection under her care, to Mariana Picasso and Diego Montalti from the Museo de La Plata for their trust in accessing the materials, to María Florencia Sosa for checking the English grammar, to Alejandra Piro and Jorge La Grotteria for their help and support in preparing the manuscript, to G. Mayr, J. Watanabe, one anonymous reviewer and the editor M. Päckert for their helpful comments.

References

- Bateson W (1894) Materials for the study of variation, treated with especial regard to discontinuity in the origin of species. Macmillan, London.
- Baumel JJ, Witmer LM (1993) Osteologia. In: Baumel JJ, King SA, Breazile JE, Evans HE, Berge JC (Eds) Handbook of Avian Anatomy: *Nomina anatomica avium*. Publications of the Nuttall Ornithological Club, Cambridge, 45–132.
- Bellairs Ad'A, Jenkin CR (1960) The skeleton of birds. In: Marshall AJ (Ed.) Biology and Comparative Physiology of Birds. Academic Press, New York and London, 241–300. <https://doi.org/10.1016/b978-1-4832-3142-6.50012-4>
- Böhmer C, Amson E, Arnold P, van Heteren AH, Nyakatura JA (2018) Homeotic transformations reflect departure from the mammalian ‘rule of seven’ cervical vertebrae in sloths: Inferences on the Hox code and morphological modularity of the mammalian neck. *BMC Evolutionary Biology* 18: 1–11. <https://doi.org/10.1186/s12862-018-1202-5>
- Bornstein PE, Peterson RR (1966) Numerical variation of the presacral vertebral column in three population groups in North America. *American Journal of Physical Anthropology* 25: 139–146. <https://doi.org/10.1002/ajpa.1330250205>
- Bumpus HC (1897) A contribution to the study of variation. *Journal of Morphology* 12: 455–484. <https://doi.org/10.1002/jmor.1050120207>
- Burke AC, Nelson CE, Morgan BA, Tabin C (1995) Hox genes and the evolution of vertebrate axial morphology. *Development* 121: 333–346. <https://doi.org/10.1242/dev.121.2.333>
- Cimen M, Elden H (1999) Numerical variations in human vertebral column a case report. *Okajimas Folia Anatomica Japonica* 75: 297–303. https://doi.org/10.2535/ofaj1936.75.6_297
- Danforth CH (1930) Numerical variation and homologies in vertebrae. *American Journal of Physical Anthropology* 14: 463–481. <https://doi.org/10.1002/ajpa.1330140311>
- de Beer Kaufman P (1974) Variation in the number of presacral vertebrae in Bantu-speaking South African Negroes. *American Journal of Physical Anthropology* 40: 369–374. <https://doi.org/10.1002/ajpa.1330400308>
- Decker HR (1915) Report of the anomalies in a subject with a supernumerary lumbar vertebra. *Anatomical Record* 9: 181–189. <https://doi.org/10.1002/ar.1090090203>
- Felice RN, O’Connor PM (2014) Ecology and caudal skeletal morphology in birds: The convergent evolution of pygostyle shape in underwater foraging taxa. *PLoS One* 9: e89737. <https://doi.org/10.1371/journal.pone.0089737>
- Fürbringer M (1888) Untersuchungen zur Morphologie und Systematik der Vögel: zugleich ein Beitrag zur Anatomie der Stütz- und Bewegungsorgane. T. van Holkema, Amsterdam.
- Gadow HF (1933) The Evolution of the Vertebral Column. Cambridge University Press, Cambridge.
- Galbusera F (2018) The spine: Its evolution, function, and shape. In: Galbusera F, Wilke HJ (Eds) Biomechanics of the Spine: Basic Concepts, Spinal Disorders and Treatments. Academic Press, New York, NY, 3–9. <https://doi.org/10.1016/b978-0-12-812851-0.00001-x>
- Galbusera F, Bassani T (2019) The spine: A strong, stable, and flexible structure with biomimetics potential. *Biomimetics* 4: 60. <https://doi.org/10.3390/biomimetics4030060>
- Galis F (1999) Why do almost all mammals have seven cervical vertebrae? Developmental constraints, Hox genes, and cancer. *Journal of Experimental Zoology* 285: 19–26. [https://doi.org/10.1002/\(sici\)1097-010x\(19990415\)285:1<19::aid-jez3>3.3.co;2-q](https://doi.org/10.1002/(sici)1097-010x(19990415)285:1<19::aid-jez3>3.3.co;2-q)
- Gervais P, Alix E (1877) Osteologie et myologie des manchots ou Sphéniscids. *Journal of Zoology* 6: 424–472.
- Gofur MR (2021) Comparative Anatomy of the Domestic Animals and Birds. Noor Publications, Bangladesh.
- Gomez C, Pourquié O (2009) Developmental control of segment numbers in vertebrates. *Journal of Experimental Zoology B* 312: 533–544. <https://doi.org/10.1002/jez.b.21305>
- Guinard G, Marchand D (2010) Modularity and complete natural homeoses in cervical vertebrae of extant and extinct penguins (Aves: Sphenisciformes). *Evolutionary Biology* 37: 210–226. <https://doi.org/10.1007/s11692-010-9097-0>
- Guinard G, Marchand D, Courant F, Gauthier-Clerc M, Le Bohec C (2010) Morphology, ontogenesis and mechanics of cervical vertebrae in four species of penguins (Aves: Spheniscidae). *Polar Biology* 33: 807–822. <https://doi.org/10.1007/s00300-009-0759-2>
- Guinard G (2012) Evolutionary concepts meet the neck of penguins (Aves: Sphenisciformes), towards a “survival strategy” for evo-devo. *Theory in Biosciences* 131: 231–242. <https://doi.org/10.1007/s12064-012-0156-1>
- Hiraga T, Sakamoto H, Nishikawa S, Muneuchi I, Ueda H, Inoue M, Shimura R, Uebayashi A, Yasuda N, Momose K, Masatomi H, Teraoka H (2014) Vertebral formula in red-crowned crane (*Grus japonensis*) and hooded crane (*Grus monacha*). *Journal of Veterinary Medical Science* 76: 503–508. <https://doi.org/10.1292/jvms.13-0295>
- Jadwiszczak P (2014) At the root of the early penguin neck: A study of the only two cervicodorsal spines recovered from the Eocene of Antarctica. *Polar Research* 33: 23861. <https://doi.org/10.3402/polar.v33.23861>
- Kaiser GW (2007) The Inner Bird: Anatomy and Evolution. UBC Press, Vancouver. <https://doi.org/10.59962/9780774855686>

- Lian J, Levine N, Cho W (2018) A review of lumbosacral transitional vertebrae and associated vertebral numeration. *European Spine Journal* 27: 995–1004. <https://doi.org/10.1007/s00586-018-5554-8>
- Mallo M (2021) Of necks, trunks and tails: Axial skeletal diversity among vertebrates. *Diversity* 13: 289. <https://doi.org/10.3390/d13-070289>
- Narita Y, Kuratani S (2005) Evolution of the vertebral formulae in mammals: A perspective on developmental constraints. *Journal of Experimental Zoology B* 304: 91–106. <https://doi.org/10.1002/jez.b.21029>
- Nickel R, Schummer A, Seiferle E (1977) *Anatomy of the Domestic Bird*. Verlag Paul Parey, Berlin.
- Ono K (1980) Comparative osteology of three species of Japanese cormorants of the genus *Phalacrocorax* (Aves, Pelecaniformes). *Bulletin of the National Science Museum Series C (Geology & Paleontology)* 6: 129–151.
- Oostra RJ, Hennekam RC, de Rooij L, Moorman AF (2005) Malformations of the axial skeleton in Museum Vrolijk I: Homeotic transformations and numerical anomalies. *American Journal of Medical Genetics A* 134: 268–281. <https://doi.org/10.1002/ajmg.a.30639>
- Pereira A (2015) Análise osteológica do Pinguim-de-Magalhães *Spheniscus magellanicus* (Forster, 1781). Universidade Federal do Rio Grande do Sul, Porto Alegre.
- Sawin PB, Gow M, Muehlke M (1967) Morphogenetic studies of the rabbit. XXXVII. Genome, gradient growth pattern and malformation. *American Journal of Anatomy* 121: 197–216. <https://doi.org/10.1002/aja.1001210203>
- Schultz AH (1947) Variability in man and other primates. *American Journal of Physical Anthropology* 5: 1–14. <https://doi.org/10.1002/ajpa.1330050102>
- Shufeldt RW (1901) Osteology of the penguins. *Journal of Anatomy and Physiology* 35: 390.
- Simoens P, Vos ND, Lauwers H, Nicaise M (1983) Numerical vertebral variations and transitional vertebrae in the goat. *Anatomia, Histologia, Embryologia* 12: 97–103. <https://doi.org/10.1111/j.1439-0264.1983.tb01006.x>
- Sosa MA, Acosta Hospitaleche C (2022) Postnatal ontogeny of the spine of the emperor penguin *Aptenodytes forsteri* (Aves, Sphenisciformes) and modularity of the neck. *Polar Biology* 45: 309–329. <https://doi.org/10.1007/s00300-021-02986-2>
- Sridevi P, Rajalakshmi K, Sivakumar M, Karthikeyan A (2021) Gross morphological studies on the vertebral column of Indian eagle owl (*Bubo bengalensis*). *Indian Journal of Animal Research* 55: 801–805. <https://doi.org/10.18805/ijar.b-4132>
- Stephan B (1979) Vergleichende Osteologie der Pinguine. *Mitteilungen aus dem Zoologischen Museum in Berlin* 3: 3–98. <https://doi.org/10.1002/mmz.4830550302>
- Takashima Y, Mizuma Y (1981) The comparison of skeletons of chicken, Japanese quail and chicken-quail hybrid. *Tohoku Journal of Agricultural Research* 32: 139–145.
- Verheyen R (1955) La systématique des Anseriformes basée sur l'ostéologie comparée (suite). *Bulletin de l'Institut Royal des Sciences Naturelles de Belgique* 36: 1–16.
- Verheyen R (1958a). Convergence ou paramorphogenèse. Systématique et phylogénie des manchots (Sphenisciformes). *Gerfaut* 48: 43–69.
- Verheyen R (1958b) Note sur la classification des Procellariiformes (Tubinares). *Bulletin de l'Institut Royal des Sciences Naturelles de Belgique* 30: 1–22.
- Verheyen R (1960) Considerations sur la colonne vertébrale des oiseaux (non-passeres). *Bulletin de l'Institut Royal des Sciences Naturelles de Belgique* 36: 1–24.
- Watson M (1883) Report on anatomy of the Spheniscidae collected during the voyage of H.M.S. Challenger. In: Murray J (Ed.) *Report of the Scientific Results of the Voyages of H.M.S. Challenger During the Years 1872–76. Part 18 (Zoology), Volume 7*. Published by Order of Her Majesty's Government, London, Edinburgh, Glasgow and Dublin, 1–244, plates 1–19.

Supplementary Material 1

Table S1

Authors: Sosa MA, Acosta Hospitaleche C (2024)

Data type: .pdf

Explanation notes: Specimens of the six species analyzed, the number of vertebrae and the association of the synsacrum to the pelvic girdle. Abbreviation: fl: indicates the number of vertebrae fused to form the pygostyle.

Copyright notice: This dataset is made available under the Open Database License (<http://opendatacommons.org/licenses/odbl/1.0>). The Open Database License (ODbL) is a license agreement intended to allow users to freely share, modify, and use this dataset while maintaining this same freedom for others, provided that the original source and author(s) are credited.

Link: <https://doi.org/vz.74.e114112.suppl1>